Articles

Potent Inhibition of Grb2 SH2 Domain Binding by Non-Phosphate-Containing Ligands

Zhu-Jun Yao,[‡] C. Richter King,[§] Tin Cao,[§] James Kelley,[‡] George W. A. Milne,[‡] Johannes H. Voigt,[‡] and Terrence R. Burke, Jr.*[,‡]

Laboratory of Medicinal Chemistry, Division of Basic Sciences, National Cancer Institute, National Institutes of Health, Bethesda, Maryland 20892, and Lombardi Cancer Center, Georgetown University Medical Center, Washington, D.C.

Received June 26, 1998

Development of Grb2 Src homology 2 (SH2) domain binding inhibitors has important implications for treatment of a variety of diseases, including several cancers. In cellular studies, inhibitors of Grb2 SH2 domain binding have to date been large, highly charged peptides which relied on special transport devices for cell membrane penetration. Work presented in the current study examines a variety of pTyr mimetics in the context of a high-affinity Grb2 binding platform. Among the analogues studied are new non-phosphorus-containing pTyr mimetics **23a** and **23b** which, when incorporated into tripeptide structures **18f** and **20f**, are able to inhibit Grb2 SH2 domain binding with affinities among the best yet reported for non-phosphorus-containing SH2 domain inhibitors (IC_{50} values of 6.7 and 1.3 μM, respectively). The present study has also demonstrated the usefulness of the *N*α-oxalyl group as an auxiliary which enhances the binding potency of both phosphorus- and non-phosphorus-containing pTyr mimetics. When combined with the (phosphonomethyl)phenylalanine (Pmp) residue to give analogues such as **L-20d**, potent inhibition of Grb2 SH2 domain binding can be achieved both in extracellular assays using isolated Grb2 SH2 domain protein and in intracellular systems measuring the association of endogenous Grb2 with its cognate $p185^{erbB-2}$ ligand. These latter effects can be achieved at micromolar to submicromolar concentrations without prodrug derivatization. The oxalyl-containing pTyr mimetics presented in this study should be of general usefulness for the development of other Grb2 SH2 domain antagonists, independent of the β-bend-mimicking platform utilized for their display.

Introduction

Signal transduction is critical to normal cellular homeostasis, with aberrations in some signaling pathways having potentially adverse effects, including the promotion of cancers and immune disorders. The phosphotyrosyl pharmacophore (pTyr, **1**) serves a central role in protein-tyrosine kinase (PTK)-mediated signal transduction by providing key recognition features necessary for assembly of multicomponent signaling complexes through the actions of Src homology 2 (SH2), phosphotyrosine-binding (PTB), and newly discovered[1] "STYX" domains.[2] For SH2 domains, recognition of pTyr-containing ligands frequently depends on interaction of the pTyr phosphate with two arginine residues in a well-formed pocket. Additional, secondary binding interactions are also provided by amino acids 2−3 residues C-proximal to the pTyr residue, which introduce differential affinity toward SH2 domain subfamilies.[3] Development of SH2 domain inhibitors has therefore concerned itself with three thematic areas: (1) interactions within the pTyr binding pocket,[4] (2) interactions with recognition areas outside the pTyr pocket, and (3) bridging elements between structural features 1 and 2.[5,6]

In the first area of investigation, pTyr mimetics have been sought which are stable to phosphatases and which offer the potential for cell membrane penetration. Phosphonate-based pTyr mimetics, such as (phosphonomethyl)phenylalanine (Pmp, **2**)[7] and (difluorophosphonomethyl)phenylalanine (F_2Pmp, **3**),[8] which replace the tyrosyl phosphate ester bond with a methylene unit, can retain good SH2 domain binding affinity in extracellular preparations,[9,10] and when administered into cells by microinjection[11] or cell permeabilization techniques,[12] they have been shown to exhibit effects consistent with SH2 domain inhibition. However, while useful for pharmacological studies, such delivery techniques do not hold promise for in vivo studies. A more traditional approach using prodrug derivatization of the phosphonate moiety has met with limited success when applied to F_2Pmp-containing peptides.[13] These considerations have led to the examination of non-phosphorus-containing pTyr

* To whom correspondence should be addressed at: Bldg 37, Rm 5C06, National Institutes of Health, Bethesda, MD 20892. Phone: (301) 496-3597. Fax: (301) 402-2275. E-mail: tburke@helix.nih.gov.
‡ National Institutes of Health.
§ Georgetown University Medical Center.

10.1021/jm980388x
Published on Web 12/05/1998

mimetics,[4,14,15] including *O*-malonyltyrosine (OMT, **4**)[16] and fluoro-*O*-malonyltyrosine (FOMT, **5**),[17] which may offer alternative approaches to cell delivery. The present study was undertaken to examine the application of known pTyr mimetics such as F_2Pmp and Pmp as well as new pTyr mimetics, in the context of Grb2 (growth factor receptor bound protein 2)[18] SH2 domain binding systems, with a particular emphasis on cell-based studies without the need of prodrug derivatization.

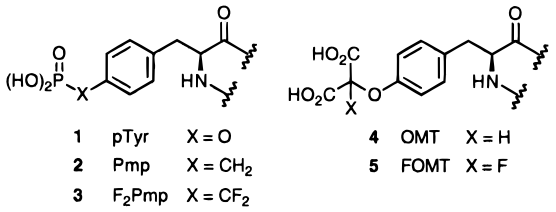

Synthesis

pTyr-containing β-bend mimetic **18b** is within the structural family of Grb2 SH2 domain antagonists previously synthesized by solid-phase techniques.[19,20] Despite repeated attempts, we were unable to achieve the synthesis of **18b** by solid-phase methods while maintaining the N-terminal naphthylpropylamide. This failure was most probably related to steric crowding induced by the naphthylpropylamido group proximal to the α-amino and carboxyl moieties of the β-bend-forming 1-aminocyclohexanecarboxylic acid residue (**13**). All syntheses were therefore conducted by solution methods. Key naphthylpropylamine-containing dipeptide **14** was prepared by reacting amine **11** with the *N*-hydroxysuccinimide active ester of *N*-Boc-L-asparagine to yield the corresponding amide **12**. The required naphthylpropylamine **11** has previously been reported;[21] however it was found expeditious to prepare it by the alternate route shown in Scheme 1.[22]

Scheme 1

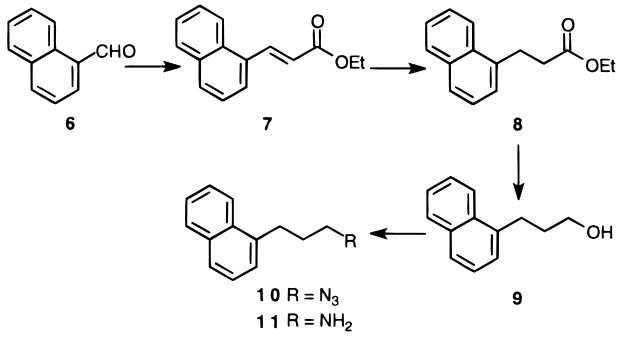

After deprotection of **12a** to amine **12b**, coupling with *N*-Boc-1-aminocyclohexanecarboxylic acid (**13**) provided the protected dipeptide **14a** (Scheme 2). Free dipeptide amine **14b**, obtained upon standard N-deprotection, was coupled with Tyr (**15a**), pTyr (**15b**), or pTyr mimetics **15c**,[23] **15d**,[24] **15e**,[25] or **15f**,[25] all bearing suitable protecting groups.

Removal of amino protection and acetylation gave the corresponding *N*-acetyl analogues **17a**−**f**, which after cleavage of remaining protecting groups and HPLC purification, gave final tripeptides **18a**−**f** (Scheme 3).

Scheme 2

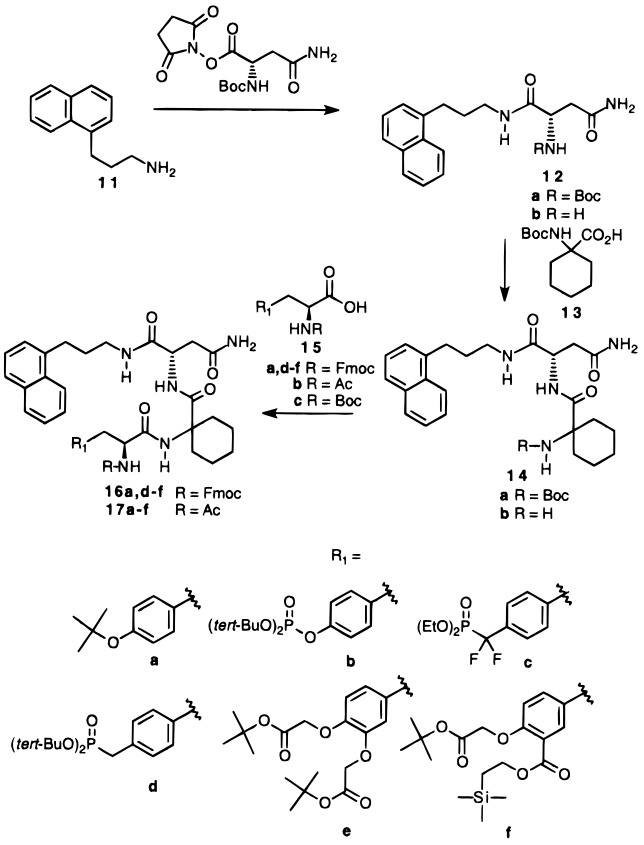

Of note was tripeptide **17f**, which required removal of the 2-trimethylsilylethyl ester (tetrabutylammonium fluoride) prior to TFA treatment.[25] Synthesis of oxalyl-containing analogues **20d** and **20f** was identical to that described for analogues **18d** and **18f**, respectively,

Scheme 3

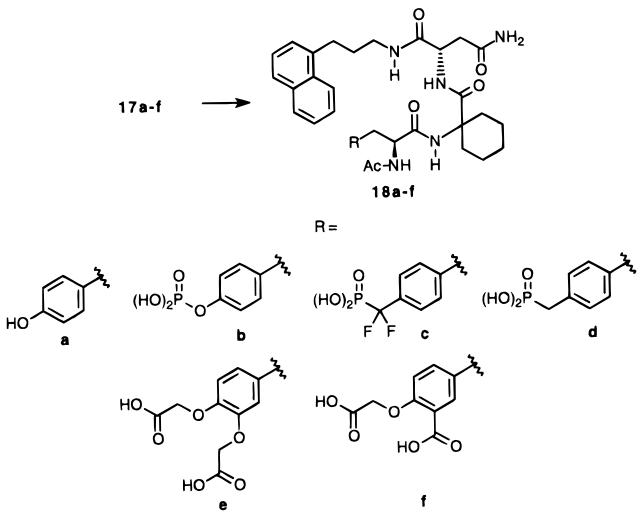

except that N-acylation with *tert*-butyl oxylate was performed rather than acetylation (Scheme 4).

Results and Discussion

The present work examines non-phosphate-containing pTyr mimetics in the context of Grb2 SH2 domain

Scheme 4

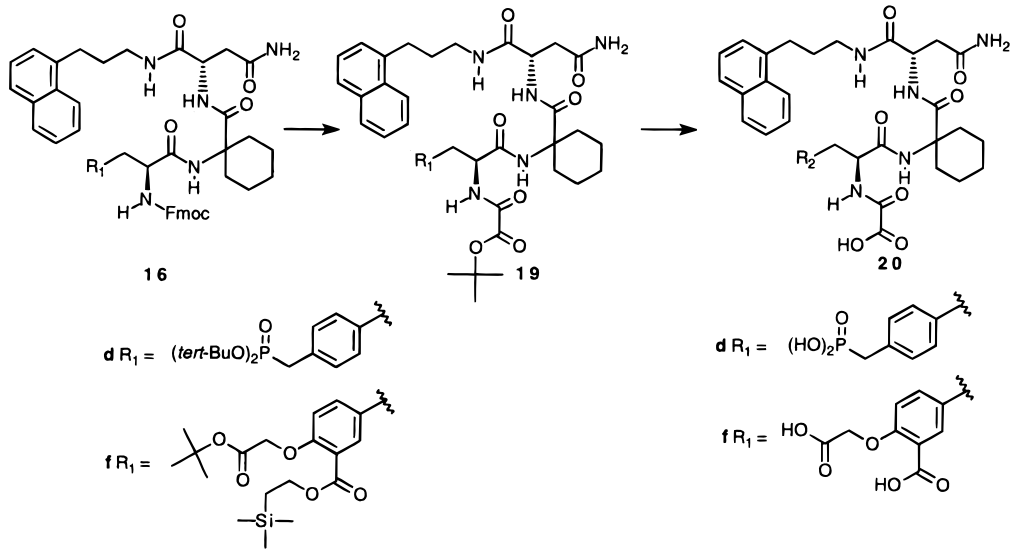

binding systems. The Grb2 SH2 domain affords an ideal target for such a study because it provides critical links between growth factor receptor PTKs and downstream signaling events involving Ras proteins, which have been directly implicated with oncogenic processes. Examples of this include members of the epidermal growth factor receptor (EGFR) PTK family such as ErbB-2 (HER-2/neu), which are found in a large proportion of breast cancers,[26] the Met (hepatocyte growth factor/scatter factor) PTK, which is overexpressed in many human tumors,[27] and the Bcr-Abl PTK, which is necessary for Philadelphia chromosome-positive leukemia.[28,29] There is a significant overexpression of mRNA for ErbB-2 in many breast cancers, with an associated increase in the levels of its phosphorylated gene product, p185^{erbB-2}. In experimental cell systems such an overexpression of p185^{erbB-2} leads to cell transformation,[30,31] and signaling via Grb2 has also been shown to be sufficient to transform such cells.[32,33] Blockade of Grb2 SH2 domain binding could potentially provide a means of uncoupling p185^{erbB-2} from the Ras pathway and, in so doing, attenuate its transforming effects. Accordingly, oblation of Grb2 function, either by elimination of the entire Grb2 protein through antisense polynucleotides[28] or by competitive blockade of Grb2 SH2 domain binding interactions with pTyr-containing peptides,[34,35] can inhibit cell growth or EGF-induced Ras/mitogen-activated protein kinase signaling, respectively.

A Novartis group has accordingly reported several high-affinity pTyr-containing ligands, which, in addition to having in common a pTyr residue that binds in the pTyr pocket and an Asn residue in the pTyr + 2 position, contain other features that enhance Grb2 binding affinity.[36] Among these features are elements which induce β-bend conformations, as shown by cyclic peptide **21** ($IC_{50} = 0.37\ \mu M$)[37] and β-bend-mimicking open-chain tripeptides typified by **22** ($IC_{50} = 0.011\ \mu M$)[19,20] which utilize a 1-aminocyclohexanecarboxylic acid in the pTyr + 1 position to facilitate β-bend formation.[38] This latter type of structure provided an ideal starting point for the current study, which is focused on interactions within the pTyr binding pocket.

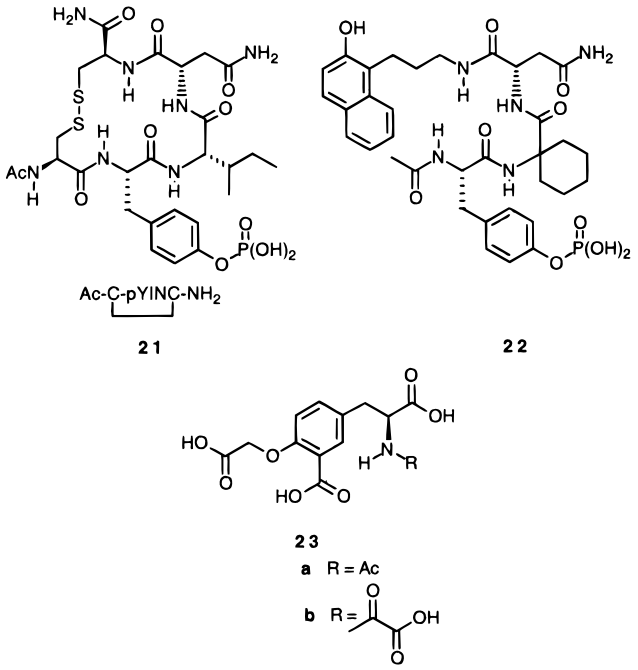

Plasmon Reasonace Binding Studies. To examine pTyr mimetics in the context of Grb2 SH2 inhibitors, the recently disclosed high-affinity pTyr-containing tripeptide **18b**[19,20] was chosen as a model platform on which to append phosphotyrosyl-mimicking analogues. A series of new inhibitors **18c**−**f**, **20d**, and **20f** incorporating pTyr mimetics **15c**−**f** was prepared, and Grb2 SH2 domain binding affinities were determined by surface plasmon reasonance (Figures 1 and 2).[39,40] The linear Shc(Y317) peptide D-D-P-S-pY-V-N-V-Q (**24**) was employed as a reference and gave an IC_{50} of 1.3 μM in this system. Consistent with previous reports,[19,20] the parent pTyr-containing **18b** also exhibited very potent binding affinity ($IC_{50} = 0.07\ \mu M$). The importance of the "phosphate pharmacophore" to the overall binding of **18b** was confirmed by the loss of all measurable binding affinity upon removal of the phosphate group (compound **18a**).

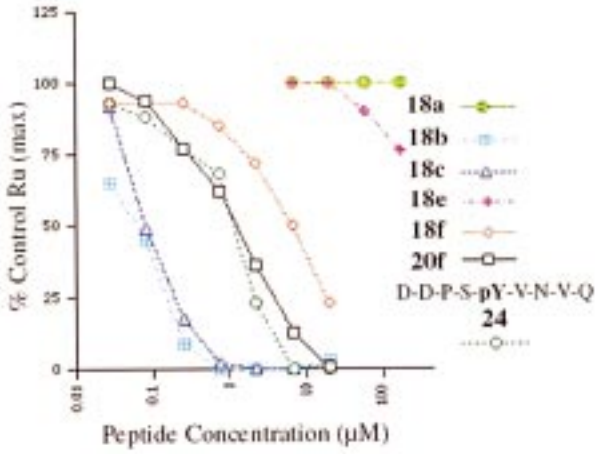

Figure 1. Effect of tyrosine modification on inhibition of Grb2 SH2 domain binding. Recombinant GST-Grb2 SH2 domain was mixed with the compounds indicated, and the mixture was allowed to flow across the surface-bound SHC phosphopeptide. The amount of equilibrium binding (Ru(max)) was determined and compared to binding when no inhibitor is present. As a control, the SHC phosphopeptide sequence (D-D-P-S-pY-V-N-V-Q) was used. Unmodified tyrosine (**18a**) shows no inhibitory activity. The most potent inhibitors contained phosphate (**18b**) and phosphonate (**18c**).

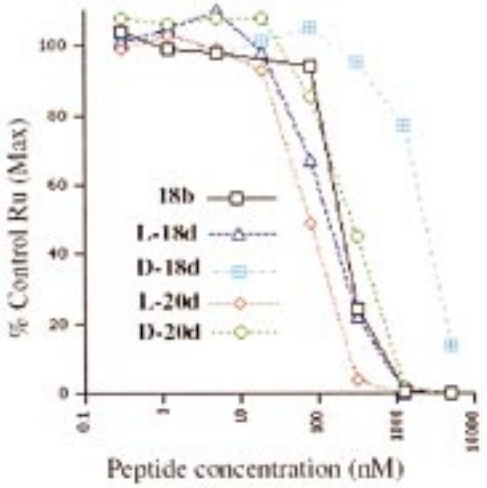

Figure 2. Effect of stereochemistry and *N*α-oxalyl modification on inhibition of Grb2 SH2 domain binding. Recombinant GST-Grb2 SH2 domain was mixed with the compounds indicated, and the mixture was allowed to flow across the surface-bound SHC phosphopeptide. The amount of equilibrium binding (Ru(max)) was determined and compared to binding when no inhibitor is present. As a control the phosphorylated **18b** was used. The most potent compound was the L-enantiomer of the *N*α-oxalyl-modified phosphonate (**L-20d**).

Experiments were conducted with phosphonate-containing analogues. The difluorophosphonate-based analogue **18c** ($IC_{50} = 0.08\ \mu M$) was found to be equally potent to the pTyr-containing parent, which contrasts with the previous demonstration of a 5-fold reduction in potency in a Grb2 SH2 domain binding system for a linear F_2Pmp-containing peptide relative to its pTyr-containing homologue.[10] The nonfluorinated phosphonate-containing compound **L-18d**[41] showed inhibitory potency equivalent to that of the F_2Pmp-containing **18c**, which is also somewhat unexpected, since for other SH2 domain systems, Pmp-containing analogues frequently show reduced inhibitory potency.[10,14,42] The reasons for the unexpectedly high potency of the Pmp-containing inhibitor are not obvious. Also seen in Figure 2 is the marked loss of potency for the D-Pmp-containing compound **D-18d**[41] relative to its L-counterpart.

Carboxylate-based pTyr mimetics were examined next. Non-phosphorus-containing pTyr mimetics such as OMT (**4**) were originally designed to afford structural alternatives to phosphorus-containing pTyr mimetics.[16] In the current study, analogues **18e** and **18f** were envisioned to function as variants of OMT in which one malonyl carboxyl has been replaced with a hydrogen, while the second carboxyl has been translocated to a more distal location. Retention of two carboxyl groups was deemed necessary in order to provide a dianionic "phosphate pharmacophore" that could interact with two critical arginines within the pTyr binding pocket. As seen in Figure 1, appending the second carboxyl to a flexible side chain resulted in a dramatic loss of binding affinity (**18e**, $IC_{50} \gg 100\ \mu M$). Anchoring the second carboxyl directly onto the aryl ring resulted in significantly better affinity (**18f**, $IC_{50} = 6.7\ \mu M$).

The reduced binding potency of **18f** relative to phosphate-containing analogue **18b** could potentially indicate that interactions of the two carboxyls of **18f** with Arg67 (αA-helix) and Arg86 (βC-strand) within the pTyr binding pocket do not faithfully approximate that provided by the phosphorus-containing parent structure **18b**. Note was therefore taken of the fact that the tyrosyl α-nitrogen provides a site from which additional critical interaction with Arg67 can be derived.[36] To examine whether introduction of anionic functionality onto the tyrosyl α-nitrogen could allow beneficial interaction with the positively charged Arg67 residue, pTyr mimetic **23a** was modified by appending an *N*α-oxalyl group to yield tricarboxylic analogue **23b**. A conceptually similar approach has been used in the design of a phosphorylated 2-(phenylmethyl)succinic acid pTyr mimetic.[43] Figure 3C depicts the results of a molecular dynamics simulation examining one possible manner in which **23b** could interact with the pTyr binding pocket. Of particular note is the ability of the *N*α-oxalyl carboxyl to bind to the αA-helix Arg67. Also evident are the ways in which the aryl bis-carboxyls of **23b** can provide key recognition features displayed by the parent phosphate group (Figure 3A). Introduction of mimetic **23b** into the general β-bend-mimicking platform was achieved in straightforward fashion by N-terminal acylation using *tert*-butyl oxylate prior to final TFA-mediated deprotection. Consistent with modeling expectations, increased binding affinity was observed (**20f**, $IC_{50} = 1.3\ \mu M$). This 5-fold enhancement in affinity makes the non-phosphorus-containing **20f** equivalent in potency to the reference linear phosphopeptide **24**, which was based on the physiologically relevant Shc(Y317) sequence.

The ability of *N*α-oxalyl functionality to enhance the binding interaction of the carboxy pTyr mimetic suggested that *N*α-oxalyl functionality could potentially have benefitial effects on Pmp-containing inhibitors. Molecular modeling dynamics simulations of *N*α-oxalyl Pmp-containing **20d** in the pTyr binding pocket showed that while maintaining key binding interactions of the pTyr-containing **18b**, significant new interactions between the Arg67 residue and elements of the *N*α-oxalyl

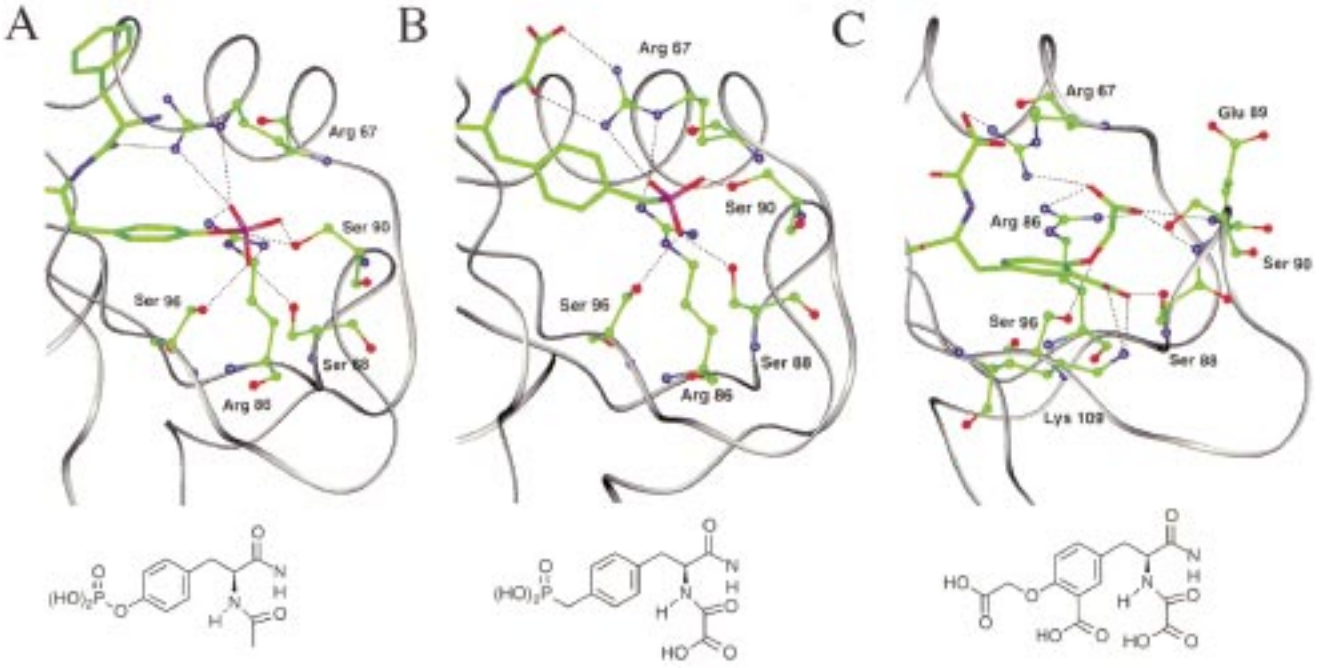

Figure 3. Interactions within the pTyr-binding pocket of ligated Grb2 SH2 domain, with particular note to interactions with Arg67. (A) X-ray structure of bound KPFpYVNV peptide.[47] Binding of the pTyr residue (truncated after the Phe residue) is shown with water molecules omitted. (B) Binding of the *N*α-oxalyl L-Pmp residue used for compound **20d**. (C) Binding of the *N*α-oxalyl residue **23b** used in compound **20f**. Structures shown in panels B and C were derived as described in the Experimental Section.

group were evident (Figure 3A,B). These modeling predictions were consistent with plasmon reasonance binding which showed that oxalyl L-Pmp (**L-20d**)[41] binds approximately 2-fold higher affinity than **L-18d** (Figure 2). For the D-Pmp analogue (**D-20d**),[41] the enhancing effect of the *N*α-oxalyl group is even more pronounced (approximately 5-fold) relative to parent analogue **D-18d** (Figure 2).

Inhibition of Grb2 SH2 Domain Binding in Cell-Based Systems. Data in Figures 1 and 2 reflect inhibition measured using isolated Grb2 SH2 domain protein relative to a reference phopsho-SHC(Y317) peptide. In physiological contexts however, Grb2 SH2 domains exist as part of larger Grb2 proteins which bind to pTyr-containing ligands which are themselves protein in nature. To examine the ability of synthetic analogues to inhibit the interaction of native Grb2 with p185^{erbB-2}, two assays were used, one in which inhibitors were introduced directly into cell lysates and one of which required the compounds to cross membranes of intact cells. In both cases, MDA-MB-453 cells were utilized. These cells are derived from a human breast cancer where there is amplification of the *erb*B-2 gene and resultant overexpression of mRNA and protein. In these cells there is a heavily phosphotyrosinylated protein detectable by immuoblotting of cell lysates, which corresponds to the overexpressed p185^{erbB-2}.[44] Interaction of native Grb2 protein with ErbB2 was monitored by immunoprecipitating Grb2 and detecting the amount of p185^{erbB-2} which is coprecipitated using anti-phosphotyrosine Western blotting.[40] As shown in Figure 4, when F_2Pmp-containing **18c** and tricarboxy-based **20f** are introduced into MDA-MB-453 cell lysates, there is a clear dose-dependent reduction in the associated p185^{erbB-2} bound to Grb2. Consistent with plasmon reasonace binding data (Figures 1 and 2), the level of

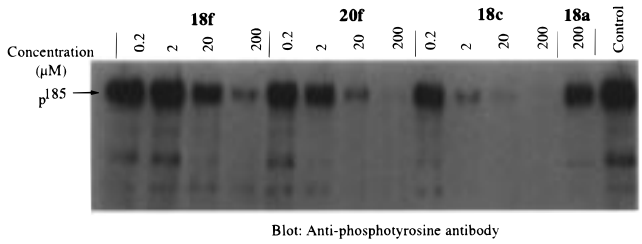

Figure 4. Inhibition of Grb2 interaction with tyrosine phosphorylated p185^{erbB-2}. Compounds showing activity in surface plasmon resonance assays were tested for their ability to inhibit interaction between intact Grb2 protein with a natural protein target, p185^{erbB-2}, in cell extracts. Cell lysates were prepared, and Grb2 was immunoprecipitated in either the presence or absence of inhibitor. Phosphotyrosinylated proteins that coimmunoprecipitate were detected by immunoblotting using specific anti-pTyr antibodies. Comparison of **18f** with **20f** shows the effect of *N*α-oxalyl modification on inhibitory activity. The phosphate requirement for **18c** is shown by the nonphosphorylated **18a**. All results were from one experiment with identical amounts of cell lysate treated.

inhibition is somewhat higher for **18c** as compared to **20f**. Removal of the oxalyl group (dicarboxy-based **18f**) resulted in a measurable loss of potency.

Compounds were also examined in a whole cell assay in which inhibition of intracellular Grb2 binding was measured following application of compounds to the media of MDA-MB-453 cells. These conditions required that compounds transit the cell membrane. As shown in Figure 5, while the nonphosphorylated tyrosyl analogue **18a** showed no measurable inhibition even at 50 μM concentration, compounds **18c**, **20f**, **18d**, and **L-20d** were able to inhibit Grb2 interaction with p185^{erbB-2}. In this assay, oxalyl L-Pmp-containing **L-20d** was clearly the most potent analogue with densiometric scanning of the blot indicating an IC_{50} value potentially as low

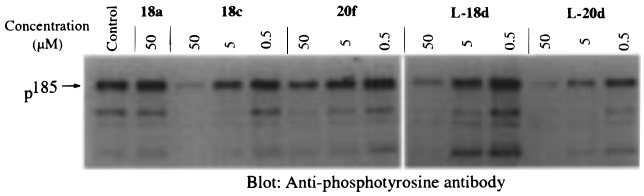

Figure 5. Interaction of Grb2 with p185^{erbB-2} can be potently inhibited. Compounds showing activity in surface plasmon resonance assays were tested for their ability to inhibit interaction between intact Grb2 protein with a cellular target by incubation of intact cells in culture. Cells were exposed to inhibitors for 3 h, washed, and lysed, and Grb2 was immunoprecipitated. pTyr-containing p185^{erbB-2} that co-immunoprecipitate were detected using specific pTyr antibodies and immuoblotting. The most potent compound was the L-enantiomer of the phosphonate bearing *N*α-oxalyl modification. All results shown were from a single experiment where plates containing the same number of cells were treated.

as 0.5 μM. Comparison of the cellular data in Figure 5 with the cell-free IC_{50} values obtained by surface plasmon reasonance shows an approximate 50-fold reduction in potency incurred by cell membrane transit. While evaluation of IC_{50} values is likely to vary with the time of exposure to the compound, the cell line, and the exact methodology used, these results suggest that oxalyl L-Pmp-containing **L-20d** is a potent inhibitor of Grb2 when applied to intact cells.

Conclusions

Development of Grb2 SH2 domain binding inhibitors has important implications for treatment of a variety of cancers. To date, Grb2 SH2 domain blockers used in cellular contexts have been large, highly charged peptides which relied on special transport devices for cell membrane penetration.[34,35,45] The work presented in the current study has focused on pTyr mimetics and their potential application to cell-based studies. New non-phosphorus-containing pTyr mimetics **23a** and **23b** have been introduced, which, when incorporated into high-affinity β-bend-mimicking platforms **18f** and **20f**, are able to exhibit Grb2 SH2 domain with low micromolar affinity. Compounds **18f** and **20f** are relatively compact, highly lipophilic molecules which represent improvements over previously reported non-pTyr-containing competitive antagonists to Grb2 SH2 domains that have utilized much larger peptide structures.[40,45,46] The present study has also demonstrated the usefulness of the *N*α-oxalyl group as an auxiliary which enhances the binding potency of both phosphorus and non-phosphorus-containing pTyr mimetics. When combined with the Pmp residue to give analogues such as **L-20d**, potent inhibition of Grb2 SH2 domain binding can be achieved in extracellular assays. More importantly, when administered to cells without prodrug derivatization, intracellular inhibition of Grb2 SH2 domain binding is achieved at micromolar to submicromolar concentrations. The oxalyl-containing pTyr mimetics presented in this study should be of general usefulness for the development of other Grb2 SH2 domain antagonists, independent of the particular β-bend-mimicking platform utilized for their display.

Experimental Section

Molecular Modeling. All simulations were performed with the Insight II 97.0/Discover 3.0 modeling package (Molecular Simulations Inc., San Diego, CA), using the cff91 force field, which was modified to take into account the planarity of the oxalylic amide group. The crystal structure of K-P-F-pY-V-N-V-NH_2 bound to Grb2 SH2[47] was used as the starting geometry. The heptapeptide within the receptor was modified appropriately to yield **20d** and **20f** in which the naphthyl group was omitted. The resulting structure of **20d** complexed to the SH2 domain was then solvated with a 20-Å sphere of water (673 molecules) centered around the spirocyclohexyl Cα of **20d.** After 300 steps of energy minimization with the Polak−Ribiere conjugated gradient algorithm (CG-PR), 50 ps of an NVT molecular dynamics simulation (MD) at 298 K was performed. The coordinates were saved every 1.0 ps. During minimization and simulation, all atoms were held fixed except **20d**, the water molecules within a 15-Å sphere about the spirocyclohexyl Cα of **20d**, and the side chains of the Grb2 SH2 protein within 5 Å around the initial conformation of the heptapeptide. The lowest-energy structure out of the 50 saved frames was minimized with 3 steps of steepest decent (SD) and 115 steps of CG-PG and is displayed in Figure 3B. For **20f**, the structure of the protein−peptide complex was subjected to a quenched molecular dynamics simulation (QMD, NVT ensemble) at 800 K. The coordinates were saved every 200 fs and minimized by 300 steps of CG-PR. During the simulation, all atoms except the side chain of the pTyr were held fixed. For the nonbonding interactions, a cutoff of 1.0 Å, a spline width of 1.0 Å, and a buffer width of 0.5 Å were used. The resulting 300 structures were grouped into 19 clusters with an rmsd cutoff of 0.8 Å, and the representative structures for each of the 19 clusters were sorted by energy. The five lowest-energy structures displayed a similar mode of binding. The next five structures again showed a similar mode of binding, which was different from the one of the first group. The lowest-energy structure of each group was solvated with 687 and 670 water molecules, respectively, and subjected to MD in the same way as **20d**. The total energy without solvent molecules for the lowest-energy frames of both MD runs was compared after minimization with 1 step of SD and 144 steps of CG-PR minimization for the first group and 1 step of SD and 151 steps of CG-PR minimization for the second group without applying constraints in both cases. For the structure from the first group, a lower energy was obtained, and this complex is displayed in Figure 3C. A constant dielectric constant of 1.00 and the cell multipole method with fine accuracy were used for all nonbonding interactions except from the QMD.

Biological. A. Inhibition of SH2 Domain Binding Using Surface Plasmon Resonance (SPR). The methods used were designed to measure a solution IC_{50} for peptide inhibition of the Grb2 SH2 domain. The approach minimizes the "left shift" encountered in SPR experiments that is observed when binding equilibrium constants are determined from association and dissociation rates at the SPR surface. In this study the SPR serves simply as a detector of free Grb2 SH2 in solution. The IC_{50} values are determined by mixing peptide with recombinant Grb2 SH2 domains and then measuring the amount of binding at equilibrium to the immobilized SHC phosphopeptide. The methods were essentially as previously described for the quantitative comparison of binding constants for the binding of other SH2 domains with phosphopeptides in solution.[39] In our experiments the immobilized phase was generated using SHC phosphopeptide, biotin-DDPSpYVNVQ (Quality Controlled Biochemicals, QCB), >90% purity by C_{18} HPLC and of the appropriate molecular weight (1453) by mass spectrometry. This peptide was attached to SA5 chips at 2 nM. Binding of GST-Grb2 was conducted at 200 nM in HBS buffer (20 mM Tris (pH 7.4), 150 mM NaCl, 0.01% Triton X-100) at flow rate of 5 μL/min for 10 min. Total Ru change for GST-Grb2 SH2 binding to SHC phosphopeptide in the absence of inhibitors was 150−250 Ru. Compounds tested as inhibitors at the indicated concentrations were premixed with the GST-Grb2 SH2 prior to introduction onto the immobilized chip monitored. The SHC phosphopeptide, DDPSpYVN-VQ, was obtained from QCB. Equilibrium binding Ru was determined at 20 s following the last GST-Grb2 SH2 flowing

across the chip. Two experiments were conducted using separate sensor chips and peptide dilutions.

B. Inhibition of Grb2 SH2 Domain Binding in Cell Extracts. Cell lysates were prepared from serum-treated *erb*B-2-overexpressing breast (MDA-MB-453) cancer cells using 1% Triton X-100 in PBS containing 0.2 mM $NaVO_4$. Lysates were incubated with the indicated concentration of inhibitory compounds for 30 min. Grb2 and associated Grb2-binding proteins were immunoprecipitated from each lysate (5 mg) with anti-Grb2 antibodies and collected using protein A Sepharose using methods previously described.[48] Immunoprecipitated proteins were separated by SDS−PAGE on 8−16% gradient gels (Novagen). pTyr-containing proteins were detected by Western blotting using anti-phosphotyrosine antibodies (Upstate Biochemicals Inc.). Previous experiments have shown that a major tyrosine phosphorylated protein in these cells is the $p185^{erbB-2}$, which is overexpressed as a consequence of gene amplification.[44]

C. Inhibition of Grb2 SH2 Domain Binding in Whole Cells. MDA-MB-453 cells were treated with the indicated compounds of for 3 h in serum-free media, IMEM (Gibco). Cells were washed twice with PBS to remove the inhibitory compound. To determine the amount of phosphotyrosine-bound $p185^{erbB-2}$, cells were then treated as described described above; cells were lysed, Grb2 was immunoprecipitated, and phosphotyrosine-containing proteins were detected using immunoblotting and anti-phosphotyrosine antibody.

Synthesis. General Synthetic Methods. Elemental analyses were obtained from Atlantic Microlab Inc., Norcross, GA, and fast atom bombardment mass spectra (FABMS) were acquired with a VG Analytical 7070E mass spectrometer under the control of a VG 2035 data system. Where indicated, FABMS matrixes used were glycerol (Gly) or nitrobenzoic acid (NBA): ^{1}H NMR data were obtained on a Bruker AC250 spectrometer (250 MHz) and are reported in ppm relative to TMS and referenced to the solvent in which they were run. Solvent was removed by rotary evaporation under reduced pressure, and silica gel chromatography was performed using Merck silica gel 60 with a particle size of 40−63 μm. Anhydrous solvents were obtained commercially and used without further drying. Preparative HPLC were conducted using a Waters Prep LC4000 system having photodiode array detection.

Ethyl 3-(Naphth-1-yl)prop-2-enoate (7). To a suspension of NaH (60% in mineral oil, 2.4 g, 60 mmol) in anhydrous ether (200 mL) was slowly added a solution of triethyl phosphonoacetate (12.33 g, 55 mmol) in anhydrous ether (25 mL) over 30 min at 0 °C, and the mixture was stirred at 0 °C (1 h). A solution of 1-naphthaldehyde (**6**) (90−95%; 8.44 g, ∼54 mmol) in ether (25 mL) was added, and the reaction was allowed to warm to room temperature and then stirred (8 h). After an extractive aqueous workup, the resulting organic layers were dried (Na_2SO_4) and solvent removed to provide **7** as a colorless oil[49] (12.47 g, quantitative based on aldehyde): ^{1}H NMR ($CDCl_3$) δ 8.62 (1H, d, J = 15.9 Hz), 8.29 (1H, d, J = 8.1 Hz), 7.97 (2H, m), 7.85 (1H, d, J = 7.1 Hz), 7.54−7.70 (3H, m), 6.62 (1H, d, J = 15.9 Hz), 4.41 (1H, q, J = 7.1 Hz), 1.47 (3H, t, J = 7.1 Hz).

Ethyl 3-(Naphth-1-yl)propanoate (8). A solution of **7** (12 g, 53.1 mmol) in 95% EtOH (180 mL) was hydrogenated over 10% Pd/C (600 mg) at room tempeature using an H_2-filled balloon (overnight). The reaction mixture was filtered and taken to dryness to give a **8** as a clear oil[50] (11.9 g, 98%): ^{1}H NMR ($CDCl_3$) δ 8.05 (1H, d, J = 7.8 Hz), 7.86 (1H, dd, J = 2.7, 7.6 Hz), 7.75 (1H, d, J = 7.6 Hz), 7.35−7.58 (4H, m), 4.17 (2H, q, J = 7.1 Hz), 3.44 (2H, t, J = 8.1 Hz), 2.77 (2H, t, J = 8.3 Hz), 1.26 (3H, t, J = 7.1 Hz).

3-(Naphth-1-yl)propan-1-ol (9). To a suspension of $LiAlH_4$ (1.91 g, 50.4 mmol) in anhydrous ether (50 mL) was added dropwise a solution of **8** (11.5 g, 50.4 mmol) in ether (50 mL) over 30 min at 0 °C, under argon and then the mixture was stirred at room temperature (overnight). The reaction mixture was cooled to 0 °C and quenched by slow (30 min) addition of H_2O (7.2 mL, 0.4 mol); then the mixture was stirred at 0 °C (1 h). Solid was removed by filtration and washed with ether; then the combined ether solution was dried (Na_2SO_4) and taken to dryness, yielding **9** as an oil[51] (9.36 g, 100%): ^{1}H NMR ($CDCl_3$) δ 8.08 (1H, dd, J = 2.4, 7.4 Hz), 7.88 (1H, m), 7.74 (1H, d, J = 7.6 Hz), 7.34−7.57 (4H, m), 3.76 (2H, t, J = 6.4 Hz), 3.20 (2H, t, J = 7.5 Hz), 2.05 (2H, m), 1.75 (1H, brs).

3-(Naphth-1-yl)propyl 1-Azide (10). To a solution of **9** (9.0 g, 48.4 mmol) in anhydrous CH_2Cl_2 (100 mL) were added MsCl (4.5 mL, 58.1 mmol) and triethylamine (10.1 mL, 72.6 mmol) under argon at 0 °C. The mixture was stirred first at 0 °C (2 h) and then at room temperature (30 min) and then subjected to an aqueous extractive workup. The resulting organic layer was dried (Na_2SO_4) and taken to dryness to provide crude **10** (12.55 g, 98%). This was taken up in dry DMF (100 mL), stirred with sodium azide (3.78 g, 58.1 mmol) at 90 °C (3 h), then cooled to room temperature, and poured into ice−water (200 mL). The mixture was extracted with dichloromethane (3 × 50 mL), washed with brine (100 mL), dried (Na_2SO_4), and taken to dryness. The residue was purified by silica gel chromatography using a mixture of hexanes and ethyl acetate (20:1, v/v) to afford **10** as a clear oil (8.38 g, 82% based on the alcohol **9**): ^{1}H NMR ($CDCl_3$) δ 8.04 (1H, dd, J = 1.5, 7.8 Hz), 7.88 (1H, dd, J = 2.2, 7.4 Hz), 7.76 (1H, d, J = 8.0 Hz), 7.33−7.58 (4H, m), 3.39 (2H, t, J = 6.7 Hz), 3.19 (2H, t, J = 7.4 Hz), 2.06 (2H, m).

3-(Naphth-1-yl)propylamine (11). To a solution of **10** (1.19 g, 5.63 mmol) in anhydrous ether (20 mL) was added a solution of $LiAlH_4$ in THF (1 M, 6 mL, 6 mmol) under argon at 0 °C. The reaction mixture was stirred at room temperature (1 h), quenched at 0 °C by addition of 1 N aqueous NaOH (0.86 mL), then stirred (1 h; 0 °C), and filtered through a pad of Celite. The filtrate was dried (Na_2SO_4) and taken to dryness to provide **11** as a clear oil (1.04 g, 100%):[21,22] ^{1}H NMR (DMSO) δ 8.09 (1H, dd, J = 2.0, 7.3 Hz), 7.90 (1H, dd, J = 2.4, 7.0 Hz), 7.75 (1H, d, J = 7.8 Hz), 7.34−7.57 (4H, m), 3.06 (2H, t, J = 7.8 Hz), 2.62 (2H, t, J = 6.9 Hz), 1.72 (2H, tt, J = 6.9, 8.0 Hz), 1.50 (2H, brs).

3-(Naphth-1-yl)propanamido-*N*-(*tert*-butoxycarbonyl)-L-asparagine (12a). Freshly prepared amine **11** (525 mg, 2.84 mmol) and *N*-Boc-L-Asn *N*-hydroxysuccinimide ester (935 mg, 2.84 mmol) in anhydrous dimethoxyethane (10 mL) were stirred at room temperature. The reaction mixture solidified after 10 min and was allowed to stand (1 h) and then treated with cold H_2O (30 mL). The resulting white solid was collected by filtration, washed with H_2O (5 × 10 mL), and dried in vacuo to provide **12a** in a quantitative yield: ^{1}H NMR (DMSO) δ 8.12 (1H, d, J = 7.3 Hz), 7.94 (2H, m), 7.80 (1H, d, J = 7.3 Hz), 7.43−7.62 (4H, m), 7.32 (1H, s), 6.93 (2H, m), 4.26 (1H, dt, J = 7.1, 6.9 Hz), 3.20 (2H, dt, J = 6.3, 6.1 Hz), 3.07 (2H, t, J = 7.5 Hz), 2.45 (2H, m), 1.83 (2H, tt, J = 7.3, 7.1 Hz), 1.41 (9H, s); FABMS (+VE, Gly) m/z 400 (MH^+).

Compound 14a. A solution of **12a** (398 mg, 1 mmol) in 10% (v/v) TFA in dichloromethane (11 mL) was stirred at room temperature (overnight); then solvent was removed and residue dried under vacuum to give crude amine **12b** as its TFA salt. An active ester solution prepared by stirring *N*-Boc-1-amino-1-cyclohexanecarboxylic acid (**13**) (243 mg, 1 mmol), HOBT·H_2O (153 mg, 1 mmol), and dicyclohexylcarbodiimide (DCC) (240 mg, 1.15 mmol) in anhydrous DMF (3 mL) at room temperature (30 min) was added to a solution of **12a**·TFA and diisopropylethylamine (DIPEA) (0.348 mL, 2 mmol) in DMF (2 mL), and the reaction mixture was stirred at room temperature (overnight). Solvent was removed under high vacuum, and the residue was chromatographed over silica gel using first EtOAc:$CHCl_3$ (1:10) and then MeOH:$CHCl_3$ (1:10) to provide **14a** as a white foam (353 mg, 67% based on **12a**): ^{1}H NMR (DMSO) δ 8.08 (2H, m), 7.90 (1H, m), 7.75 (1H, m), 7.62 (1H, m), 7.50 (2H, m), 7.39 (3H, m), 7.27 (1H, s), 6.92 (1H, s), 4.38 (1H, m), 3.45 (1H, m), 3.24 (1H, m), 3.03 (2H, t, J = 6.7 Hz), 2.73 (1H, m), 2.44 (1H, dd, J = 5.1, 16.1 Hz), 1.69−2.05 (6H, m), 1.40−1.65 (6H, m), 1.34 (9H, s); FABMS (+VE, Gly) m/z 525 (MH^+).

General Procedure for the Synthesis of Compounds 16a and 16d−f. Treatment of **14a** with TFA:triethylsilane

(100: 2) at room temperature (1 h) and removal of TFA provided **14b**·TFA, which was partitioned between aqueous $NaHCO_3$ and EtOAC to provide free amine **14b** [FABMS (+VE, Gly) *m*/z 425 $[M + H]^+$; HRMS calcd for $C_{24}H_{33}N_4O_3$ (MH^+) *m*/z 425.2552, found 425.2557]. To a solution of **14b** (106 mg, 0.25 mmol) in anhydrous DMF (1 mL) was added an active ester solution formed by reacting appropriately protected pTyr mimetic **15a**, **15d**,[24] **15e**,[25] or **15f**[25] (0.3 mmol), HOBT·H_2O (41 mg, 0.3 mmol), and DIPCDI (47 μL, 0.3 mmol) in anhydrous DMF (0.5 mL) at room temperature (10 min). The combined reaction mixture was then stirred at room temperature overnight. Solvent was removed under high vacuum, and residue was purified by silica gel chromatography (EtOAc in $CHCl_3$) to provide products as white foams. Compound **16a**: 90% yield; FABMS (+VE, NBA) *m*/z 866 (MH^+). Compound **16d**: 69% yield (an unresolved mixture of diastereomers, epimeric at the Pmp α-carbon); FABMS (+VE, NBA) *m*/z 982.8 (MH^+). Compound **16e**: 79% yield; FABMS (+VE, NBA) *m*/z 1054.6 (MH^+). Compound **16f**: 79% yield; FABMS (+VE, NBA) *m*/z 1068.3 (MH^+).

General Procedure for Conversion of Compounds 16a and 16d−f to Their *N*-Acetyl Derivatives 17a and 17d−f, Respectively. To solutions of **16a** and **16d−f** (0.1−0.2 mmol) in anhydrous MeCN (2.0 mL) was added piperidine (4 equiv), and the solutions were stirred at room temperature (1 h). Solvent and excess piperidine were removed under high vacuum; then residues were taken up in anhydrous MeCN and treated with *N*-acetylimidazole (4 equiv) at room temperature. After all amine had reacted (from 3 to 24 h) solvent was removed, and residues were purified by silica gel chromatography (EtOAc in $CHCl_3$) to provide pure products as resins in quantitative yield, except where noted. Compound **17a**: FABMS (+VE, Gly) *m*/z 686 (MH^+); HRMS calcd for $C_{39}H_{52}N_5O_6$ *m*/z 686.3918 $[M + H]^+$, found 686.3882. Compound **L-17d**: faster, 29% yield.[41] Compound **D-17d**: slower, 18% yield.[41] Compound **17e**: FABMS (+VE, NBA) *m*/z 874.6 (MH^+). Compound **17f**: FABMS (+VE, NBA) *m*/z 885.5 (MH^+).

Compound 17b. A solution of **14a** (168 mg, 0.320 mmol) in 20% (v/v) TFA in dichloromethane (3.6 mL) was stirred at room temperature (overnight); then solvent was removed and residue was dried to give crude **14b**·TFA as a syrup. An active ester solution formed by reacting *N*-Ac-L-Tyr((*tert*-BuO)$_2$PO)-OH (146 mg, 0.352 mmol), HOBT·H_2O (54 mg, 0.352 mmol), and DCC (73 mg, 0.352 mmol) in DMF (1 mL) (20 min) was added to a solution of **14b**·TFA and DIPEA (0.113 mL, 0.64 mmol) in DMF (2 mL), and the reaction mixture was stirred at room temperature (7 h). Solvent was removed under high vacuum and the residue was chromatographed on silica gel, elueting with MeOH:$CHCl_3$ (1:40, 1:20, then 1:10) to provide **L-17b**[41] as a white foam (60.4 mg). Also obtained was the diastereomer **D-17b**[41] (29 mg) resulting from partial racemization at the tyrosyl α-carbon. Additionally, an unseparated mixture of **L-17b** and **D-17b** (79.2 mg) was collected, providing a 64% combined yield of tyrosyl-coupled product. **L-17b**: ^{1}H NMR (DMSO) δ 8.22 (2H, m), 8.10 (1H, m), 7.97 (1H, d, J = 8.1 Hz), 7.89 (1H, m), 7.74 (1H, m), 7.49 (3H, m), 7.37 (3H, m), 7.21 (2H, d, J = 8.5 Hz), 7.03 (2H, d, J = 8.3 Hz), 6.90 (1H, s), 4.60 (1H, m), 4.35 (1H, m), 3.16 (2H, m), 3.03 (4H, m), 2.73 (1H, t, J = 11.4 Hz), 2.59 (1H, dd, J = 6.6, 11.9 Hz), 1.75 (3H, s), 1.43 (18H, s), 1.17−2.05 (12H, brm). **D-17b**: ^{1}HNMR (DMSO) δ 8.49 (1H, s), 8.45 (1H, d, J = 5.4 Hz), 8.09 (1H, m), 7.90 (1H, m), 7.76 (1H, t, J = 4.6 Hz), 7.65 (1H, d, J = 8.1 Hz), 7.27−7.52 (8H, m), 7.06 (2H, d, J = 8.3 Hz), 6.87 (1H, s), 4.57 (1H, m), 4.42 (1H, dt, J = 5.1, 9.3 Hz), 3.28 (1H, m), 3.05 (3H, m), 2.87 (2H, m), 2.59 (2H, m), 1.77 (3H, s), 1.43 (18H, s), 1.15−2.00 (12H, brm); FABMS (+VE, NBA) *m*/z 822 (MH^+).

Compound 17c. To a solution of amine **14b** (106 mg, 0.25 mmol) in DMF (1 mL) was added an activated ester solution formed by reacting L-*N*-Boc-F_2Pmp(OEt)$_2$−OH (**15c**)[23] (135 mg, 0.30 mmol), HOBt·H_2O (46 mg, 0.30 mmol), and DIPCDI (47 μL, 0.30 mmol) in DMF (1.0 mL) (20 min), and the combined solution was stirred at room temperature (overnight). DMF was removed under high vacuum and residue was chromatographed on silica gel ($CHCl_3$:MeOH, 25:1) to provide the Boc-protected tripeptide as a white foam (197 mg, 92%): ^{1}HNMR (DMSO, 250 MHz): δ 8.20 (1H, s), 8.00−8.15 (2H, m), 7.90 (1H, m), 7.73 (1H, m), 7.36−7.50 (10H, m), 7.21 (1H, d, J = 7.3 Hz), 6.91 (1H, s), 4.36 (2H, m), 4.10 (4H, m), 3.38−3.50 (2H, m), 3.17 (2H, m), 3.04 (2H, t, J = 7.8 Hz), 2.66 (2H, m), 1.35−2.10 (12H, m), 1.30 (9H, s), 1.21 (3H, t, J = 7.1 Hz), 1.20 (3H, t, J = 7.1 Hz).

A portion of this material (130 mg, 0.152 mmol) in dichloromethane (1 mL) with TFA (1 mL) was stirred at room temperature (1 h); then solvent was removed. The resulting foam was dissloved in DMF (1 mL) containing triethylamine (46 μL, 0.334 mmol) and 1-acetylimidazole (25 mg, 0.230 mmol), and the mixture was stirred at room temperature (2 h) and then concentrated. Chromatographic purification of the residue on silica gel ($CHCl_3$:MeOH, 15:1) provided **17c** as a white foam (122 mg, 100%): ^{1}H NMR (DMSO) δ 8.25 (1H, m), 7.87−8.13 (4H, m), 7.74 (1H, t, J = 4.9 Hz), 7.36−7.53 (10H, m), 6.91 (1H, s), 4.70 (1H, m), 4.36 (1H, m), 6.91 (1H, s), 4.70 (1H, m), 4.36 (1H, m), 4.09 (4H, m), 3.41−3.52 (2H, m), 3.16 (2H, m), 3.04 (2H, t, J = 8.0 Hz), 2.56−2.63 (2H, m), 1.74 (3H, s), 1.20 (6H, t, J = 7.1 Hz), 1.15−2.01 (12H, m).

Final Product 18a. A solution of **17a** (0.21 mmol) in TFA (1.9 mL) with H_2O (0.1 mL) and triethylsilane (50 μL) was stirred at room temperature (1 h), then taken to dryness, and purified by HPLC using a Prep NovaPak HR C_{18} 6-μm radial compression cartridge (200 mm × 40 mm diameter) with a flow rate of 50 mL/min and a linear gradient from 10% to 50% B over 20 min (solvent A, 0.1% aqueous TFA; solvent B, 0.1% TFA in MeCN). Product **18a** was obtained as a white solid (118 mg, 88% yield): ^{1}H NMR (DMSO) δ 8.12−8.23 (3H, m), 7.93−8.00 (2H, m), 7.80 (1H, dd, J = 4.3, 4.7 Hz), 7.54 (3H, m), 7.43 (3H, m), 7.00−7.50 (1H, br), 7.07 (2H, d, J = 7.5 Hz), 6.94 (1H, s), 6.67 (2H, d, J = 7.5 Hz), 4.58 (1H, m), 4.40 (1H, m), 2.94−3.29 (5H, m), 2.55−2.79 (3H, m), 2.05−1.10 (12H, m), 1.81 (3H, s); FABMS (+VE, Gly) *m*/z 630 (MH^+); HR-FABMS calcd for $C_{35}H_{44}N_5O_6$ (MH^+) *m*/z 630.33292, found 630.3339.

Compound 18b. A solution of **L-17b** (48.7 mg, 0.059 mmol), thioanisole (0.100 mL), TFA (0.5 mL), and dichloromethane (0.5 mL) was stirred at room temperature (overnight), then solvent was evaporated, and the residue was dried under vacuum. The crude product was dissolved in MeCN:water (1:1, 2 mL), filtered, and purified by HPLC, using a Vydac C_{18} column (250 mm × 20 mm diameter) with a flow rate of 20 mL/min and a linear gradient from 10% to 100% B over 40 min (solvent A, 0.1% aqueous TFA; solvent B, 0.1% TFA in MeCN). Product **18b** was obtained as a white solid (26 mg, 62%): ^{1}H NMR (DMSO) δ 8.22 (2H, m), 8.07 (1H, m), 7.91 (2H, m), 7.74 (1H, m), 7.36−7.53 (6H, m), 7.17 (2H, d, J = 8.3 Hz), 7.03 (2H, d, J = 8.3 Hz), 6.90 (1H, s), 4.64 (1H, m), 4.35 (1H, m), 3.17 (3H, m), 2.72 (1H, m), 2.59 (1H, m), 1.76 (3H, s), 1.13−2.07 (12H, m) ppm; FABMS (−VE, Gly) *m*/z 708 (M − H); HR-FABMS calcd for $C_{35}H_{43}N_5O_9P$ (M − H) *m*/z 708.2798, found 708.2803.

Compound 18c. A mixture of **17c** (70 mg, 0.088 mmol), TFA (1.2 mL), thioanisole (140 μL, 1.2 mmol), TMSBr (155 μL, 1.2 mmol), and *m*-cresol (92 μL, 0.876 mmol) was stirred at room temperature (24 h); then the mixture was concentrated under argon and treated with cold ether:hexane (1:1; 7 mL) to provide a precipitate. Supernatant was removed following centrifugation, and solid was washed three times by resuspension and centrifugation. The resulting solid was purified by HPLC as indicated for the purification of **18a** using a linear gradient from 5% to 50% B over 25 min to provide **18c** as a white solid (43 mg, 66%yield): ^{1}H NMR (DMSO) δ 8.29 (1H, d, J = 7.4 Hz), 8.25 (1H, s), 8.09 (1H, t, J = 6.1 Hz), 7.99 (1H, d, J = 8.1 Hz), 7.89 (1H, dt, J = 1.9, 5.4 Hz), 7.74 (1H, t, J = 4.6 Hz), 7.33−7.54 (10H, m), 6.91 (1H, s), 4.65 (1H, m), 4.33 (1H, q, J = 6.6 Hz), 3.17 (2H, m), 3.04 (3H, m), 2.81 (1H, dd, J = 13.8, 10.7 Hz), 2.65 (1H, dd, J = 6.3, 15.1 Hz), 2.56 (1H, dd, J = 4.9, 15.1 Hz), 1.77 (3H, s), 1.10−2.05 (12H, m); FABMS (−VE, Gly) *m*/z 742 (M − H).

Final Product L-18d. Treatment of **L-17d** (0.035 mmol) as described above for the preparation of **18a** and HPLC purifica-

tion of crude product as described therein provided **L-18d** as a white solid (17 mg, 69% yield):[41] ^{1}H NMR (DMSO) δ 8.27 (2H, m), 8.12 (1H, m), 8.01 (1H, d, J = 8.1 Hz), 7.94 (1H, m), 7.80 (1H, dd, J = 4.3, 4.7 Hz), 7.55 (3H, m), 7.43 (3H, m), 7.18 (4H, m), 6.96 (1H, s), 4.67 (1H, m), 4.41 (1H, m), 3.23 (2H, m), 3.08 (3H, m), 2.94 (2H, d, J = 21.4 Hz), 2.55−2.85 (3H, m, partially covered by DMSO peaks), 1.11−2.25 (12H, m), 1.80 (3H, s); FABMS (−VE, Gly) m/z 706 (M − H); HR-FABMS calcd for $C_{36}H_{45}N_5O_8P$ (M − H) m/z 706.3006, found 706.2960.

Final Product D-18d. Treatment of **D-17d** (0.035 mmol) as described above and HPLC purification of crude product as described therein provided **D-18d** as a white solid (14 mg, 84% yield):[41] ^{1}H NMR (DMSO) δ 8.57 (1H, s), 8.47 (1H, d, J = 5.1 Hz), 8.15 (1H, m), 7.95 (1H, m), 7.81 (1H, dd, J = 4.2, 4.7 Hz), 7.66 (1H, d, J = 8.1 Hz), 7.56 (2H, m), 7.45 (3H, m), 7.34 (1H, s), 7.24 (4H, m), 6.95 (1H, s), 4.62 (1H, m), 4.47 (1H, m), 3.34 (2H, m), 2.82−3.15 (3H, m), 2.95 (2H, d, J = 21.4 Hz), 2.50−2.75 (3H, m), 1.84 (3H, s), 0.75−2.18 (12H, m); FABMS (−VE, Gly) m/z 706 (M − H); HR-FABMS calcd for $C_{36}H_{45}N_5O_8P$ (M − H) m/z 706.3006, found 706.3057.

Final Product 18e. Treatment of **17e** (0.20 mmol) as described above for the synthesis of **18a** and HPCL purification of crude product as described therein provided pure **18e** as a white solid (114 mg, 75% yield): ^{1}H NMR (DMSO) δ 8.23 (2H, m), 8.12 (1H, m), 7.93−8.00 (2H, m), 7.79 (1H, t, J = 4.3 Hz), 7.53 (3H, m), 7.42 (3H, m), 6.93 (2H, s), 6.78 (2H, s), 4.71 (2H, s), 4.68 (2H, s), 4.58 (1H, m), 4.38 (1H, m), 3.20 (2H, m), 3.08 (2H, t, J = 6.4 Hz), 2.95 (1H, dd, J = 13.7, 2.4 Hz), 2.73 (1H, dd, J = 13. 6, 10.3 Hz), 2.63 (2H, t, J = 5.4 Hz), 1.82 (3H, s), 1.10−2.05 (12H, m); FABMS (−VE, Gly) m/z 760 (M − H); HR-FABMS calcd for $C_{39}H_{46}N_5O_{11}$ (M − H) m/z 760.3194, found 760.3155.

Final Product 18f. A solution of **17f** (0.075 mmol) and tetrabutylammonium fluoride (TBAF) (1.0 M in THF, 300 μL) in anhydrous DMF (2 mL) was stirred at room temperature (overnight) and then taken to dryness under high vacuum. Residue was dissolved in a mixture of TFA (1.9 mL), H_2O (0.1 mL), and triethylsilane (50 μL), stirred at room temperature (1 h), then taken to dryness, and purified by HPLC using a Prep NovaPak HR C_{18} 6-μm radial compression cartridge (200 mm × 40 mm diameter) as described above for **18a** and **18e** to provide **18f** as its mono-TBAF salt (36 mg) and di-TBAF salt (17 mg). A portion (16 mg) of mono-TBAF salt was repurified by HPLC to provide **18f** as its free diacid (11 mg): ^{1}H NMR (DMSO) δ 8.34 (1H, s), 8.24 (1H, d, J = 6.8 Hz), 8.11 (1H, m), 8.02 (1H, d, J = 8.1 Hz), 7.95 (1H, m), 7.78 (1H, m), 7.70 (1H, s), 7.54 (3H, m), 7.34−7.43 (4H, m), 6.95 (1H + 1H, d + s, J = 8.5 Hz), 4.79 (2H, s), 4.64 (1H, m), 4.40 (1H, m), 3.40 (2H, m, partially covered by water peak), 3.22 (1H, m), 3.00−3.10 (3H, m), 2.50−2.80 (2H, m, partially covered by DMSO), 1.79 (3H, s), 2.05−1.1 (12H, m); FABMS (−VE, Gly) m/z 730 (M − H); HR-FABMS calcd for $C_{38}H_{44}N_5O_{10}$ (M − H) m/z 730.3088, found 730.2997.

Compound 19d. A mixture of diastereomers epimeric at the Pmp α-carbon (**16d**) (150 mg, 0.15 mmol) was treated with piperidine (48 μL, 0.45 mmol) in acetonitrile (2 mL) at room temperature (2 h), then solvent was removed, and residue was dried under high vacuum. At this stage a portion of crude product was purified by silica gel chromatography ($CHCl_3$:MeOH, 20:1 to 15:1) to afford two diastereomeric free amines, the L-Pmp-containing compound followed by the D-Pmp-containing coumpound.[41] For the L-Pmp-containing isomer: ^{1}H NMR (DMSO) δ 8.18 (1H, s), 8.08 (2H, m), 7.90 (1H, m), 7.75 (1H, m), 7.64 (1H, m), 7.50 (2H, m), 7.41 (3H, m), 7.01−7.12 (4H, m), 6.92 (1H, s), 4.36 (1H, m), 3.51 (1H, m), 2.90−3.27 (5H, m, partially covered by water peak), 2.94 (2H, d, J = 21.3 Hz), 2.50−2.75 (3H, m, partially covered by DMSO), 1.35 (18H, s), 1.10−2.00 (12H, m); FABMS (+VE, Gly) m/z 800 (M + Na), 778 (MH^+), 722 ($MH^+ - C_4H_8$). For the D-Pmp-containing isomer: ^{1}H NMR (DMSO) δ 8.32 (1H, s), 8.09 (2H, m), 7.89 (1H, m), 7.74 (1H, m), 7.64 (1H, m), 7.44−7.55 (3H, m), 7.40 (1H, s), 7.38 (1H, d, J = 1.7 Hz), 7.06−7.15 (4H, m), 6.97 (1H, s), 4.35 (1H, m), 3.52 (1H, m), 3.18 (2H, m), 3.05 (2H, t, J = 7.6 Hz), 2.95 (2H, d, J = 21.5 Hz), 2.85 (1H, dd, J = 1.2, 13.7 Hz), 2.72 (1H, dd, J = 4.6 13.7 Hz), 2.67 (2H, m, partially covered by DMSO), 1.35 (18H, s), 1.05−2.04 (12H, m).

The crude product (0.15 mmol) was then dissolved in DMF (1 mL) containing DIEA (44 μL, 0.25 mmol) and *tert*-butyloxalyl chloride (0.23 mmol) (prepared by reaction of oxalyl chloride with *tert*-butyl alcohol). After 10 min the reaction mixture was concentrated and purified by silica gel chromatography ($CHCl_3$:MeOH, from 30:1 to 20:1) to provide L-Pmp-containing diastereomer **L-19d** (59.4 mg, 44%) (assignment of L-Pmp configuration was based on analogy to the *N*-acetyl compound **L-17d**), followed by the D-Pmp-containing diastereomer **D-19d** (52.3 mg, 39%). For **L-19d**: ^{1}H NMR (DMSO) δ 8.69 (1H, d, J = 8.1 Hz), 8.32 (1H, s), 8.08 (1H, m), 7.97 (1H, d, J = 7.8 Hz), 7.89 (1H, m), 7.74 (1H, t, J = 4.8 Hz), 7.49 (3H, m), 7.38 (3H, m), 7.16 (4H, m), 6.92 (1H, s), 4.63 (1H, m), 4.38 (1H, m), 2.85−3.25 (8H, m), 2.67 (1H, dd, J = 6.8, 15.9 Hz), 2.55 (1H, dd, J = 5.4, 15.9 Hz, partially covered by DMSO peaks), 1.06−2.05 (12H, m), 1.41 (9H, s), 1.31 (18H, s); FABMS (+VE, Gly) m/z 928 (M + Na), 906 (MH^+).

Compound 19f. A solution of **16f** (88 mg, 0.082 mmol) in anhydrous MeCN (2 mL) with piperidine (27 μL, 0.33 mmol) was stirred at room temperature (1 h), then taken to dryness, and placed under high vacuum. Residue was dissolved in anydrous DMF (0.5 mL) and treated overnight with an activated ester solution formed by stirring (10 min) oxalic acid mono-*tert*-butyl ester (24 mg, 0.16 mmol), HOBT·H_2O (22 mg, 0.16 mmol), and DIPCDI (26 μL, 0.16 mmol) in anhydrous DMF (0.5 mL). Solvent was removed under high vacuum and residue purified by silica gel chromatography (MeOH in EtOAc) to provide **19f** as a syrup (45 mg, 56% yield): ^{1}H NMR ($CDCl_3$) δ 8.13 (2H, m), 7.98 (1H, m), 7.80−7.69 (2H, m), 7.60−7.27 (4H, m), 6.80 (2H, m), 6.42 (1H, bs), 5.78 (1H, bs), 4.80−4.66 (3H, m), 4.62 (2H, s), 4.50−4.40 (3H, m), 3.50−3.35 (2H, m), 3.25−3.00 (6H, m), 2.15−1.15 (14H, m), 1.56 (18H, s), 0.14 (9H, s); FABMS (+VE, NBA) m/z 975.2 (MH^+).

Final Product 20d. A solution of **L-19d** (45 mg, 0.0497 mmol) in dichloromethane (0.5 mL) with TFA (0.5 mL) and triethylsilane (20 μL) was stirred at room temperature (2 h); then the mixture was concentrated and dried under vacuum. Residue was purified by HPLC using an Advantage C_{18} 5-μm column (20 mm diameter × 250 mm) with a binary solvent mixture of A (0.1% aqueous TFA) and B (0.1% TFA in MeCN) and a linear gradient over 25 min from 5% to 60% B. Final product **L-20d** was obtained as a white solid (31 mg, 84%): ^{1}H NMR (DMSO) δ 8.77 (1H, d, J = 8.1 Hz), 8.32 (1H, s), 8.08 (1H, m), 7.97 (1H, d, J = 8.1 Hz), 7.91 (1H, m), 7.75 (1H, m), 7.50 (3H, m), 7.39 (3H, m), 7.14 (4H, m), 6.91 (1H, s), 4.68 (1H, m), 4.37 (1H, m), 3.16 (3H, m), 3.03 (3H, m), 2.89 (2H, d, J = 21.2 Hz), 2.68 (1H, dd, J = 6.3, 14.6 Hz), 2.53 (1H, dd, J = 4.9, 14.6 Hz), 1.15−2.05 (12H, m) (−COOH and $P(O)(OH)_2$ did not show); FABMS (−VE, Gly) m/z 736 [$(M - H)^-$], 692 [$(M - H - CO_2)^-$], 664 [$(M - H - CO_2 - CO)^-$], 322, 212, 79 [$(PO_3)^-$]; HR-FABMS calcd for $C_{36}H_{44}N_5O_{10}P$ (M − H) m/z 736.2748, found 736.2817.

D-20d was prepared as above from **D-19d** in 69% yield: ^{1}H NMR (DMSO) δ 8.95 (1H, d, J = 7.1 Hz), 8.45 (1H, s), 8.08 (1H, m), 7.89 (1H, m, 7.77 (1H, dd, J = 9.3, 2.4 Hz), 7.65 (1H, d, J = 7.6 Hz), 7.50 (2H, m), 7.38 (4H, m), 7.16 (4H, m), 6.91 (1H, s), 4.66 (1H, m), 4.40 (1H, m), 3.16 (2H, m), 3.02 (4H, m), 2.90 (2H, d, J = 21.5 Hz), 2.56 (2H, m), 0.94−2.08 (12H, m) (−COOH and $P(O)(OH)_2$ did not show); FABMS (+VE, Gly) m/z 738 (MH^+).

Final Product 20f. A solution of **19f** (37 mg, 0.038 mmol) in MeCN (1.0 mL) with 1.0 M TBAF in THF (0.12 mmol) was stirred at room temperature (2 days), then solvent was removed, and the residue was dried under vacuum. The resulting material was dissolved in a mixture of TFA (950 μL), H_2O (50 μL), and triethylsilane (25 μL) and stirred at room temperature (3 h), then taken to near dryness. Treatment with cold ether gave crude product as a white solid, which was dried under an argon stream and purified twice by HPLC as described above for the purification of **18f**, providing **20f** as a white solid (17 mg, 58%): ^{1}H NMR (DMSO) δ 8.79 (1H, d, J = 8.1 Hz), 8.4 (1H, s), 8.06 (1H, m), 7.98 (1H, d, J = 7.5 Hz),

7.87 (1H, m), 7.76 (1H, m), 7.68 (1H, d, J = 1.7 Hz), 7.29−7.55 (7H, m), 6.91 (2H, m), 4.72 (3H, m), 4.36 (1H, m), 2.90−3.26 (6H, m), 2.67 (2H, m), 1.14−2.05 (12H, m); FABMS (−VE, Gly) m/z 760 (M − H).

References

(1) Wishart, M. J.; Dixon, J. E. Gathering STYX: phosphatase like form predicts functions for unique protein-interaction domains. *Trends Biochem. Sci.* **1998**, *23*, 301−306.

(2) Mayer, B. J.; Gupta, R. Functions of SH2 and SH3 domains. *Protein Modules Signal Transduct.* **1998**, *228*, 1−22.

(3) Zhou, S. Y.; Cantley, L. C. Recognition and specificity in protein tyrosine kinase-mediated signaling. *Trends Biochem. Sci.* **1995**, *20*, 470−475.

(4) Burke, T. R., Jr.; Yao, Z.-J.; Smyth, M. S.; Ye, B. Phosphotyrosyl-based motifs in the structure-based design of protein-tyrosine kinase-dependent signal transduction inhibitors. *Curr. Pharm. Des.* **1997**, *3*, 291−304.

(5) Lunney, E. A.; Para, K. S.; Rubin, J. R.; Humblet, C.; Fergus, J. H.; Marks, J. S.; Sawyer, T. K. Structure-based design of a novel series of nonpeptide ligands that bind to the pp60(src) SH2 domain. *J. Am. Chem. Soc.* **1997**, *119*, 12471−12476.

(6) Pacofsky, G. J.; Lackey, K.; Alligood, K. J.; Berman, J.; Charifson, P. S.; Crosby, R. M.; Doresy, G. F., Jr.; Feldman, P. L.; Gilmer, T. M.; Hummel, C. W.; Jordan, S. R.; Mohr, C.; Shewchuk, L. M.; Sternbach, D. D.; Rodriguez, M. Potent dipeptide inhibitors of pp60c-src SH2 domain. *J. Med. Chem.* **1998**, *41*, 1894−1908.

(7) Marseigne, I.; Roques, B. P. Synthesis of new amino acids mimicking sulfated and phosphorylated tyrosine residues. *J. Org. Chem.* **1988**, *53*, 3621−3624.

(8) Burke, T. R., Jr.; Smyth, M.; Nomizu, M.; Otaka, A.; Roller, P. P. Preparation of fluoro- and hydroxy-4-phosphonomethyl-D,L-phenylalanine suitably protected for solid-phase synthesis of peptides containing hydrolytically stable analogues of O-phosphotyrosine. *J. Org. Chem.* **1993**, *58*, 1336−1340.

(9) Domchek, S. M.; Auger, K. R.; Chatterjee, S.; Burke, T. R.; Shoelson, S. E. Inhibition of SH2 domain/phosphoprotein association by a nonhydrolyzable phosphonopeptide. *Biochemistry* **1992**, *31*, 9865−9870.

(10) Burke, T. R., Jr.; Smyth, M. S.; Otaka, A.; Nomizu, M.; Roller, P. P.; Wolf, G.; Case, R.; Shoelson, S. E. Nonhydrolyzable phosphotyrosyl mimetics for the preparation of phosphatase-resistant SH2 domain inhibitors. *Biochemistry* **1994**, *33*, 6490−6494.

(11) Xiao, S.; Rose, D. W.; Sasaoka, T.; Maegawa, H.; Burke, T. R.; Roller, P. P.; Shoelson, S. E.; Olefsky, J. M. Syp (SH-PTP2) is a positive mediator of growth factor-stimulated mitogenic signal transduction. *J. Biol. Chem.* **1994**, *269*, 21244−21248.

(12) Wange, R. L.; Isakov, N.; Burke, T. R., Jr.; Otaka, A.; Roller, P. P.; Watts, J. D.; Aebersold, R.; Samelson, L. W. F2(Pmp)2-TAM-(zeta)3, a novel competitive inhibitor of the binding of ZAP-70 to the T cell antigen receptor, blocks early T cell signaling. *J. Biol. Chem.* **1995**, *270*, 944−948.

(13) Stankovic, C. J.; Surendran, N.; Lunney, E. A.; Plummer, M. S.; Para, K. S.; Shahripour, A.; Fergus, J. H.; Marks, J. S.; Herrera, R.; Hubbell, S. E.; Humblet, C.; Saltiel, A. R.; Stewart, B. H.; Sawyer, T. K. The role of 4-phosphonodifluoromethyl- and 4-phosphonophenylalanine in the selectivity and cellular uptake of SH2 domain ligands. *Bioorg. Med. Chem. Lett.* **1997**, *7*, 1909−1914.

(14) Gilmer, T.; Rodriquez, M.; Jordan, S.; Crosby, R.; Alligood, K.; Green, M.; Kimery, M.; Wagner, C.; Kinder, D.; Charifson, P.; Hassell, A. M.; Willard, D.; Luther, M.; Rusnak, D.; Sternbach, D. D.; Mehrotra, M.; Peel, M.; Shampine, L.; Davis, R.; Robbins, J.; Patel, I. R.; Kassel, D.; Burkhart, W.; Moyer, M.; Bradshaw, T.; Berman, J. Peptide inhibitors of src SH3−SH2-phosphoprotein interactions. *J. Biol. Chem.* **1994**, *269*, 31711−31719.

(15) Mehrotra, M. M.; Sternbach, D. D.; Rodriguez, M.; Charifson, P.; Berman, J. Alpha-dicarbonyls as "noncharged" arginine-directed affinity labels. Novel synthetic routes to alpha-dicarbonyl analogues of the pp60(c-src) SH2 domain-targeted phosphopeptide Ac-Tyr(OPO3H2)-Glu-Glu-Ile-Glu. *Bioorg. Med. Chem. Lett.* **1996**, *6*, 1941−1946.

(16) Ye, B.; Akamatsu, M.; Shoelson, S. E.; Wolf, G.; Giorgetti-Peraldi, S.; Yan, X. J.; Roller, P. P.; Burke, T. R. L-O-(2-malonyl)-tyrosine: A new phosphotyrosyl mimetic for the preparation of Src homology 2 domain inhibitory peptides. *J. Med. Chem.* **1995**, *38*, 4270−4275.

(17) Burke, T. R.; Ye, B.; Akamatsu, M.; Ford, H.; Yan, X. J.; Kole, H. K.; Wolf, G.; Shoelson, S. E.; Roller, P. P. 4′-O-[2-(2-fluoromalonyl)]-L-tyrosine: A phosphotyrosyl mimic for the preparation of signal transduction inhibitory peptides. *J. Med. Chem.* **1996**, *39*, 1021−1027.

(18) Margolis, B. The GRB family of SH2 domain proteins. *Prog. Biophys. Mol. Biol.* **1994**, *62*, 223−244.

(19) Fretz, H.; Furet, P.; Schoepfer, J.; Garcia-Echeverria, C.; Gay, B.; Rahuel, J.; Caravatti, G. Targeting a hydrophobic patch on the survace of the Grb2-SH2 Domain Leads to high-affinity phosphotyrosine-containing peptide ligands. 15th American Peptide Symposium, Nashville, TN, June 14−19, 1997; Abstract P422.

(20) After the submission of this manuscript, the full experimental for the work presented in ref 19 appeared in print: Furet, P.; Gay, B.; Caravatti, G.; Garcia-Escheverria, C.; Rahuel, J.; Schoepfer, J.; Fretz, H. Structure-based design and synthesis of high affinity tripeptide ligands of the Grb2-SH2 domain. *J. Med. Chem.* **1998**, *41*, 3442−3449.

(21) Mndzhoyan, A. L.; Badalyan, V. E.; Aleksanyan, R. A.; Bkhiyan, M. T. Synthesis of some beta, gamma-disubstituted propylguanidines. *Arm. Khim. Zh.* **1969**, *22*, 795−804.

(22) A more direct route to **11** has recently been reported; see ref 20.

(23) Smyth, M. S.; Burke, T. R., Jr. Enantioselective synthesis of N-Boc and N-Fmoc protected diethyl 4-phosphonodifluoromethyl-L-phenylalanine; agents suitable for the solid-phase synthesis of peptides containing nonhydrolyzable analogues of O-phosphotyrosine. *Tetrahedron Lett.* **1994**, *35*, 551−554.

(24) Burke, T. R., Jr.; Russ, P.; Lim, B. Preparation of 4-[bis(*tert*-butyl)phosphonomethyl]-N-Fmoc-DL-phenylalanine; a hydrolytically stable analogue of O-phosphotyrosine potentially suitable for peptide synthesis. *Synthesis* **1991**, *11*, 1019−1020.

(25) Burke, T. R., Jr.; Yao, Z.-J.; He, Z.; Milne, G. W. A.; Wu, L.; Zhang, Z. Y.; Voigt, J. H. Enantioselective synthesis of nonphosphorus-containing phosphotyrosyl mimetics and their use in the preparation of tyrosine phosphatase inhibitory peptides. *Tetrahedron* **1998**, *54*, 9981−9994.

(26) Dankort, D. L.; Wang, Z. X.; Blackmore, V.; Moran, M. F.; Muller, W. J. Distinct tyrosine autophosphorylation sites negatively and positively modulate neu-mediated transformation. *Mol. Cell. Biol.* **1997**, *17*, 5410−5425.

(27) Fixman, E. D.; HolgadoMadruga, M.; Nguyen, L.; Kamikura, D. M.; Fournier, T. M.; Wong, A. J.; Park, M. Efficient cellular transformation by the Met oncoprotein requires a functional Grb2 binding site and correlates with phosphorylation of the Grb2-associated proteins, Cbl and Gab1. *J. Biol. Chem.* **1997**, *272*, 20167−20172.

(28) Tari, A. M.; Arlinghaus, R.; LopezBerestein, G. Inhibition of Grb2 and Crkl proteins results in growth inhibition of Philadelphia chromosome positive leukemic cells. *Biochem. Biophys. Res. Commun.* **1997**, *235*, 383−388.

(29) Ma, G. Z.; Lu, D.; Wu, Y.; Liu, J. X.; Arlinghaus, R. B. Bcr phosphorylated on tyrosine 177 binds Grb2. *Oncogene* **1997**, *14*, 2367−2372.

(30) Di Fiore, P. P.; Pierce, J. H.; Fleming, T. P.; Hazan, R.; Ullrich, A.; King, C. R.; Schlessinger, J.; Aaronson, S. A. Overexpression of the human EGF receptor confers an EGF-dependent transformed phenotype to NIH 3T3 cells. *Cell* **1987**, *51*, 1063−1070.

(31) Hudziak, R. M.; Schlessinger, J.; Ullrich, A. Increased expression of the putative growth factor receptor p185HER2 causes transformation and tumorigenesis of NIH 3T3 cells. *Proc. Natl. Acad. Sci. U.S.A.* **1987**, *84*, 7159−7163.

(32) Ben-Levy, R.; Paterson, H. F.; Marshall, C. J.; Yarden, Y. A single autophosphorylation site confers oncogenicity to the Neu/ErbB-2 receptor and enables coupling to the MAP kinase pathway. *EMBO J.* **1994**, *13*, 3302−3311.

(33) Xie, Y. M.; Pendergast, A. M.; Hung, M. C. Dominant-negative mutants of Grb2 induced reversal of the transformed phenotypes caused by the point mutation-activated rat HER-2/Neu. *J. Biol. Chem.* **1995**, *270*, 30717−30724.

(34) Rojas, M.; Yao, S. Y.; Lin, Y. Z. Controlling epidermal growth factor (EGF)-stimulated ras activation in intact cells by a cell-permeable peptide mimicking phosphorylated EGF receptor. *J. Biol. Chem.* **1996**, *271*, 27456−27461.

(35) Williams, E. J.; Dunican, D. J.; Green, P. J.; Howell, F. V.; Derossi, D.; Walsh, F. S.; Doherty, P. Selective inhibition of growth factor-stimulated mitogenesis by a cell-permeable Grb2-binding peptide. *J. Biol. Chem.* **1997**, *272*, 22349−22354.

(36) Furet, P.; Gay, B.; GarciaEcheverria, C.; Rahuel, J.; Fretz, H.; Schoepfer, J.; Caravatti, G. Discovery of 3-aminobenzyloxycarbonyl as an N-terminal group conferring high affinity to the minimal phosphopeptide sequence recognized by the Grb2-SH2 domain. *J. Med. Chem.* **1997**, *40*, 3551−3556.

(37) Gay, B.; Furet, P.; GarciaEcheverria, C.; Rahuel, J.; Chene, P.; Fretz, H. Dual specificity of Src homology 2 domains for phosphotyrosine peptide ligands. *Biochemistry* **1997**, *36*, 5712−5718.

(38) Garcia-Echeverria, C.; Furet, P.; Gay, B.; Fretz, H.; Rahuel, P.; Schoepfer, J.; Caravatti, G. Potent antagonists of the SH2 domain of Grb2: Optimization of the X=1 position of 3-amino-Z-Tyr(PO3H2)-X+1-Asn-NH_2. *J. Med. Chem.* **1998**, *41*, 1741−1744.

(39) Morelock, M. M.; Ingraham, R. H.; Betageri, R.; Jakes, S. Determination of receptor−ligand kinetic and equilibrium binding constants using surface plasmon resonance: Application to the lck SH2 domain and phosphotyrosyl peptides. *J. Med. Chem.* **1995**, *38*, 1309−1318.
(40) Oligino, L.; Lung, F. D. T.; Sastry, L.; Bigelow, J.; Cao, T.; Curran, M.; Burke, T. R., Jr.; Wang, S. M.; Krag, D.; Roller, P. P.; King, C. R. Nonphosphorylated peptide ligands for the Grb2 Src homology 2 domain. *J. Biol. Chem.* **1997**, *272*, 29046−29052.
(41) Absolute configurations of the Pmp residues were not determined unambiguously, rather the L-configuration was assigned to the enantiomer illiciting the more potent inhibition.
(42) Mikol, V.; Baumann, G.; Keller, T. H.; Manning, U.; Zurini, M. G. M. The crystal structures of the SH2 domain of p56(lck) complexed with two phosphonopeptides suggest a gated peptide binding site. *J. Mol. Biol.* **1995**, *246*, 344−355.
(43) Shahripour, A.; Plummer, M. S.; Lunney, E. A.; Para, K. S.; Stankovic, C. J.; Rubin, J. R.; Humblet, C.; Fergus, J. H.; Marks, J. S.; Herrera, R.; Hubbel, S. E.; Saltiel, A. R.; Sawyer, T. K. Novel phosphotyrosine mimetics in the design of peptide ligands for pp60src SH2 domain. *Bioorg. Med. Chem. Lett.* **1996**, *6*, 1209−1214.
(44) Kraus, M. H.; Popescu, N. C.; Amsbough, S. C.; King, C. R. Overexpression of the EGF receptor-related proto-oncogene erbB-2 in human mammary tumor cell lines by different molecular mechanisms. *EMBO J.* **1987**, *6*, 605−610.
(45) Rojas, M.; Yao, S. Y.; Donahue, J. P.; Lin, Y. Z. An alternative to phosphotyrosine-containing motifs for binding to an SH2 domain. *Biochem. Biophys. Res. Commun.* **1997**, *234*, 675−680.
(46) After submission of this manuscript, it was reported that actinomycins are able to potently inhibit Grb2 SH2 domain binding: Nam, J.-Y.; Kim, H.-K.; Son, K.-H.; Kim, S.-U.; Kwon, B.-M.; Han, M. Y.; Chung, Y. J.; Bok, S. H. Actinomycin D, C2 and VII, inhibitors of Grb2-Shc interaction produced by streptomyces. *Bioorg. Med. Chem. Lett.* **1998**, *8*, 2001−2002.
(47) Rahuel, J.; Gay, B.; Erdmann, D.; Strauss, A.; GarciaEcheverria, C.; Furet, P.; Caravatti, G.; Fretz, H.; Schoepfer, J.; Grutter, M. G. Structural basis for specificity of GRB2−SH2 revealed by a novel ligand binding mode. *Nature Struct. Biol.* **1996**, *3*, 586−589.
(48) Sastry, L.; Lin, W. H.; Wong, W. T.; Difiore, P. P.; Scoppa, C. A.; King, C. R. Quantitative analysis of Grb2-Sos1 interaction: The N-terminal SH3 domain of Grb2 mediates affinity. *Oncogene* **1995**, *11*, 1107−1112.
(49) Allen, M. C.; Brundish, D. E.; Fullerton, J. D.; Wade, R. Tritiated peptides. Part 15. Synthesis of tritium labeled biologically active analogues of somatostatin. *J. Chem. Soc., Perkin Trans. I* **1986**, 989−1004.
(50) Condon-Gueugnot, S.; Leonel, E.; Nedelec, J. Y.; Perichon, J. Electrochemical arylation of activated olefins using a nickel salt as catalyst. *J. Org. Chem.* **1995**, *60*, 7684−7687.
(51) Searles, S. The reaction of trimethylene oxide with Grignard reagents and organolithium compounds. *J. Am. Chem. Soc.* **1951**, *73*, 124.

JM980388X